Plant, Cell and Environment (1989) **12**, 371–382

Characterization and propagation of acoustic emission signals in woody plants: towards an improved acoustic emission counter

M. T. TYREE & J. S. SPERRY Department of Botany, University of Vermont, Burlington, VT 05405, U.S.A.

Received 15 July 1988; received in revised form 21 September 1988; accepted for publication 12 December 1988

Abstract. The physics of ultrasonic acoustic emissions (AEs) was investigated for AE transmission through wood and transducers. The physical properties measured were velocity, attenuation and frequency composition of AEs produced by two sources: cavitation events in xylem and pencil lead breaks. The authors also measured the relative sensitivity of various combinations of ultrasound transducers and amplifiers to aid in the selection of a measuring system optimized for cavitation detection in woody plants. Some of the authors' conclusions are: (1) Softwoods (*Thuja, Pinus*) attenuate AEs more rapidly than hardwoods (maple, birch). (2) The velocity of AEs in wood exceeds that measured by others in water so the main medium of AE transmission must be the cellulose. (3) The strongest frequencies of AEs are in the range of 100–300 kHz. (4) Cavitation-induced AEs tend to shift to higher frequency as wood dehydration progresses. (5) One cannot determine the locus of origin of AEs from its frequency composition. (6) The frequency composition of the acoustic emissions probably cannot be determined *at all* with the sensors used because of their tendency to 'ring'. The data collected in this paper were used to aid in the design of an improved AE counter having a seven-fold increase in signal to noise ratio compared to counters previously used in our laboratory. The improved counter, model 4615 Drought Stress Monitor, is now commercially available from Physical Acoustics Corp., Princeton, NJ, U.S.A.

Key-words: acoustic emission; xylem cavitation; *Acer saccharum; Thuja occidentalis; Pinus strobus.*

Introduction

Since 1983, more than a dozen papers have appeared in the literature in which cavitation events in the xylem of crops and woody plants have been detected by the amplification of ultrasonic acoustic emissions (AEs); for example, Tyree & Dixon (1986), Tyree *et al.* (1986), Pena & Grace (1986) and Salleo & LoGullo (1986). The ultrasonic transducers used in these studies were generally model 8312 (Bruel & Kjaer, Denmark); for example, Tyree & Dixon (1983) and Sanford & Grace (1985). The ultrasonic amplifiers used were either commercial (Bruel & Kjaer model 2368) or custom made owing to the high cost of purchase. Counting circuits have generally been custom-made also because of the high cost of purchase of commercial units that were often designed with more sophisticated applications in mind (Tyree, Dixon & Thompson, 1984). The present authors are not aware of any studies which determine whether the transducers currently used are optimally sensitive for the detection of AEs in plant systems or which evaluate the design of a relatively inexpensive transducer-amplifier-filter-counter combination. In 1986, the authors approached a major manufacturer of ultrasonic equipment, Physical Acoustics Corp. (PAC), to seek funds to research and develop a low-cost commercial AE counter and transducer combination having characteristics significantly improved with respect to what is currently used in the plant sciences. Funding for this research was eventually obtained from the United States Department of Energy as part of their Small Business Innovation Research (DOE-SBIR) program. In this report, the authors present work conducted in their laboratory as part of the research and development program.

The purpose of this study was to investigate the physics of AE signal propagation in the stems of some woody plants in order to aid in the selection of the transducer with the best signal to noise ratio for the detection of cavitation-induced AEs. The physical properties investigated were: (1) the velocity of AEs in woody stems generated from pencil lead breaks; (2) the frequency composition of AEs in woody stems originating from cavitation events during the dehydration of excized stem tissue; (3) the attenuation of AEs in woody stems measured on AEs both from pencil lead breaks and from cavitation events; and (4) the measurement of the relative sensitivity of various AE transducers. This information was used to design a commercial acoustic emission counter that is optimized for the detection of ultrasonic acoustic emissions in woody plants. This new instrument, the model 4615 Drought Stress Monitor, is now available from Physical Acoustics Corp., PO Box 3135, Princeton, NJ 08540, U.S.A.

Correspondence: Dr Mel Tyree, Department of Botany, University of Vermont, Burlington, VT 05405, U.S.A.

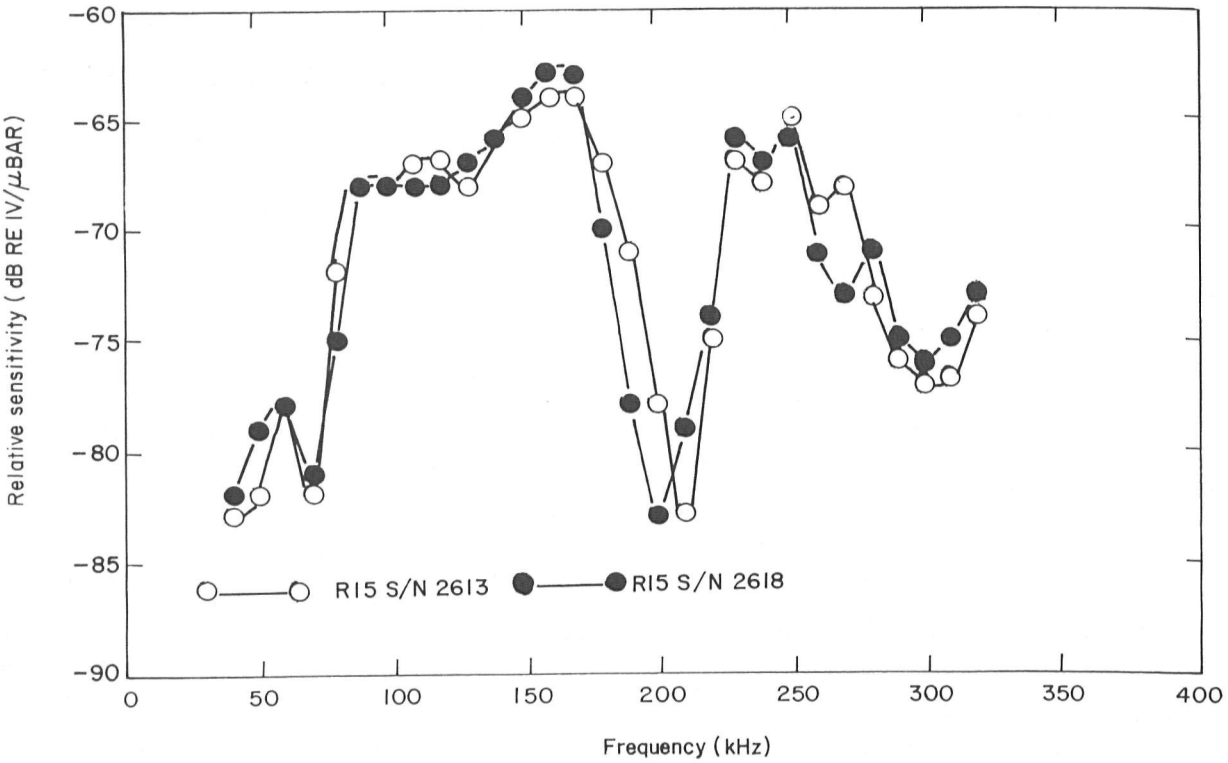

Figure 1. Frequency response of the two R15 transducers used in this study (manufacturer's data).

Materials and methods

All measurements were performed on woody samples. Most measurements were performed on living woody stem segments collected from the following trees: maple (*Acer saccharum*), *Thuja occidentalis* and pine (*Pinus strobus*). In all cases, the bark was removed and transducers were coupled to the wood medium with silicone grease in order to enhance sound transfer and to reduce localized dehydration. The transducers were held in place by spring-loaded clamps with a constant force of 30 Newtons. In some cases, measurements were performed on rectangular blocks cut from the stem segments. Some measurements were also performed on a birch dowel (probably *Betula populifolia*) of commercial lumber origin. The dowel was air dried, 90 cm long and 1.33 cm in diameter.

Velocity measurements

Velocity measurements of AEs were performed on the birch dowel and on stems of maple and pine. Two transducers (PAC model R15) were selected with nearly matched frequency responses (Fig. 1). The transducers were clamped on the same side of the stem segment or dowel at fixed spacing (usually 10 cm). Velocities were measured on AEs created by breaking a mechanical pencil lead (0.5 mm HB) a fixed distance to the right or the left of the pair of transducers. The leads were extended 3 mm beyond the tip of the mechanical pencil and broken on the surface of the wood while maintaining a contact angle of about 40°. Cavitation-induced AEs were suppressed in living wood segments by keeping one end of the stem segment in contact with water. Velocities were again measured in maple and pine samples after the stem segments were air dried.

A highly reproducible AE signal resulted from the lead break, the waveforms picked up by both transducers were very similar in shape (Fig. 2). The AE signals were amplified by a preamplifier (PAC model 1220A) and a post-amplifier (PAC model 3104). The preamplifier and post amplifiers were fitted with sixth-order band pass filters with frequency cut offs of 100 and 300 kHz. The AE signals were captured on an 8-bit waveform digitizer (Tektronix 7D20). A microcomputer (CompuPro 8-16) was in communication with the digitizer and some digital waveforms were copied and displayed on a dot matrix printer.

The time of arrival of the leading edge of the waveforms were measured directly on the oscilloscope display of the digitizer and the velocity computed from the distance between the two transducers and the difference in arrival times of the leading edges of the waveforms. The overall gain of the amplifiers were adjusted as needed to allow for signal attenuation as the waveform travelled down the wood sample. In the birch and maple samples, attenuation was small so the gain setting for the two transducers were set equal. In the pine samples,

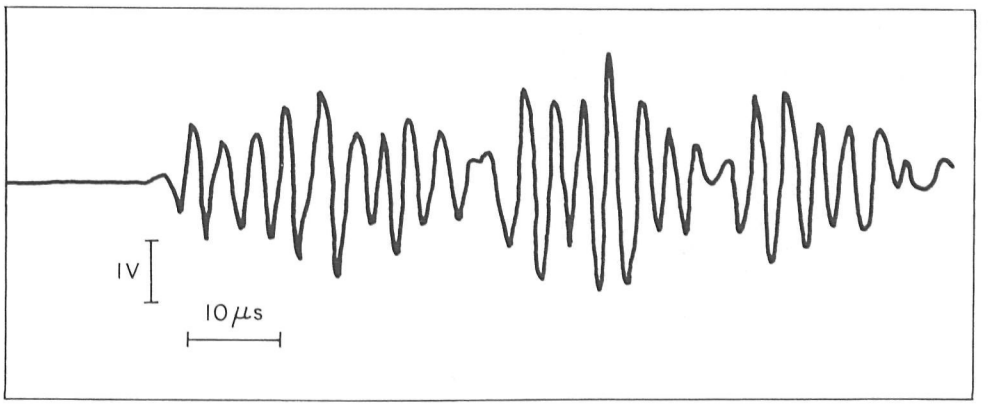

Figure 2. Typical AE signal observed for a pencil lead break on a birch dowel. The AE source was 25 cm from the R15 transducer.

attenuation was large so the gain of the transducer farthest from the AE source was set about 20 dB higher.

Acoustic emission frequency composition

Ultrasonic AEs created by cavitation events in dehydrating maple and *Thuja* samples were measured with a broad band transducer (Bruel & Kjaer model 8312). The transducer was selected at the authors' request by Bruel & Kjaer to have the flattest response of sensitivity versus frequency of all transducers produced in 1984. The calibration curve is reproduced in Fig. 3. The objective of these measurements was to determine which frequencies of cavitation-induced AEs were of largest amplitude. This permitted us to select narrow band transducers having a maximum sensitivity centred around the strongest frequency component of the cavitation-induced AEs. Although these transducers were not broad band, they do have a better signal to noise ratio.

Cavitation-induced AEs picked up by the model 8312 transducers were amplified by the internal 40 dB pre-amplifier contained in the transducer and amplified further by a Bruel & Kjaer model 2638 amplifier with an eight-order 50-kHz high-pass filter. The AEs were captured on the Tektronix 7D20 waveform digitizer and the waveforms up-loaded into a microcomputer. The sampling rate of the digitizer was 10 MHz (100 ns per voltage reading) and antialiasing filters were used. The raw waveforms (which usually represented mixtures of several frequencies) were analysed by standard discrete fast Fourier transformation (FFT) techniques to produce plots of amplitude versus frequency. The plots were then modified to account for the non-flat response of the model 8312 transducer. Frequency components in the FFT, which corresponded to frequencies where the actual sensitivity of the transducer was below the average sensitivity (horizontal line in Fig. 3), were increased in amplitude by the number of dB that the calibration curve was below the average sensitivity; similarly frequency components that were above the average sensitivity of the transducer were decreased in amplitude. Because of the limited dynamic range of the 8-bit waveform digitizer, the overall gain of the measuring system was adjusted so that only a few per cent of the AEs went beyond the full scale range of the digitizer (set to ± 5.12 V full scale). At this gain, the majority of the waveforms were below 1 volt maximum amplitude. Ultrasonic AEs below 1 volt amplitude or beyond the full scale were rejected in order to improve the accuracy of the discrete FFT analysis. All plots of amplitude versus frequency were normalized so that the maximum amplitude had a relative value of one.

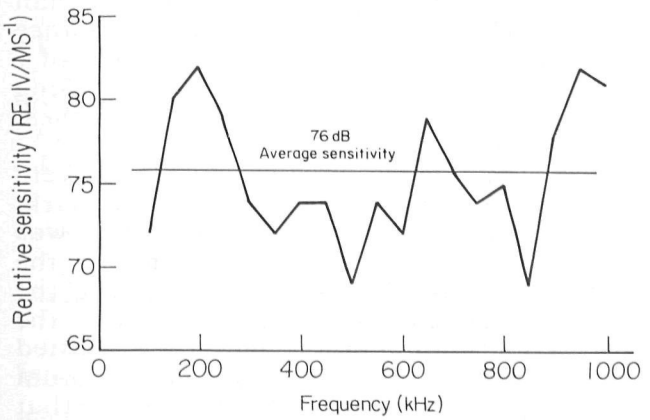

Figure 3. Frequency response of the B&K 8312 broad band transducer used in this study (manufacturer's data).

The above procedures were repeated using another broad-band transducer (Panametrics model V105). This transducer differed from the Bruel & Kjaer model 8312 in the method used to achieve broad band characteristics. The model 8312 used a very small transducer crystal having many closely spaced harmonics and the non-linear response of the crystal was partly compensated by a complementary non-linear preamplifier built into the transducer housing. The model V105 uses a large heavily damped transducer crystal designed to have a very flat

frequency response (plot of sensitivity versus frequency), and there was no built-in preamplifier. The model 8312, while broadly sensitive, tends to ring harmonically at characteristic frequencies following a 'hit' by an acoustic event in the same way that a bell struck by a hammer will ring on for a long time compared to the duration of the initiating event. The model V105 is much less sensitive than the model 8312 but it does not have strong harmonics and rings for a much shorter time.

Acoustic emission signal attenuation

Ultrasonic AE signal attenuations were measured on maple and pine samples using low-frequency and high-frequency transducers. The low-frequency measurements were made with PAC model R15 transducers having a nominal harmonic frequency of 150 kHz. The high-frequency measurements were made with PAC model R80 transducers having a nominal harmonic frequency of 800 kHz. The pre-amplifiers and post-amplifiers were PAC models 1220A and 3104, respectively. The band pass filters used were 100–300 kHz and 600–1200 kHz for the low- and high-frequency measurements, respectively.

The placement of the matched pairs of transducers were as shown in Fig. 4a for maple and birch (samples having low attenuation) and as shown in Fig. 4b for *Thuja* and pine (samples having high attenuation). Since the transducers were separated a fixed distance apart and usually unequal distances from the source of the AEs, the amplitude of the AEs received by the transducers differed because of signal attenuation. Signal attenuation, A, is defined in this study as the ratio (in dB) of maximum AE amplitude detected by the two transducers, TR1 and TR2, i.e.

$$A = (20\,\text{dB})\ \log\ [TR1/TR2] \qquad (1)$$

The amplitudes TR1 and TR2 are defined here as the maximum minus minimum voltage amplitude of the wave form (Fig. 4c).

Signal attenuations were measured for AEs of known locus of origin in the samples (i.e. a pencil lead break at a known place on the sample) and for AEs of unknown locus of origin (i.e. a cavitation event from an unknown spot in the sample).

Signal attenuations give some crude measure of the effective 'listening' distance over which AE can be detected using any given transducer. In order to relate signal attenuations between wood samples, the signal attenuation, A, was divided by the distance in centimetres that the transducers were separated. This quantity is called here the specific attenuation A_s (dB/cm). The value of A_s was easily calculated for pencil lead breaks because the source of the AE was at a known locus. For birch, maple, *Thuja* and pine samples, the transducers were arranged as shown in Fig. 4a and pencil lead breaks were to the right or left of the transducer pair.

The computation of attenuations for the cavitation-induced AEs was more complex since the locus of origin of the AEs was unknown. The amplitude of AEs from cavitation events was one or two orders of magnitude smaller than AEs from pencil lead breaks. In order to get significant numbers of coincident events in both transducers, the arrangement in Fig. 4b had to be used for *Thuja* and pine samples. Several thousand AEs were counted simultaneously in two transducers separated by a known distance, d. A histogram was constructed of the number of AEs having a signal attenuation within discrete ranges of 1 dB each. For maple samples (Fig. 4a), the histogram had two distinct peaks separated by X dB; A_s was equated to X/2d. For pine and *Thuja* samples (Fig. 4b) the histogram had one peak of width Y dB measured at the half height of the peak; A_s was equated to Y/2d. See the appendix for a discussion of how A_s was calculated for AEs from unknown loci, and for a discussion of the physical factors likely to mitigate against the accurate determination of A_s.

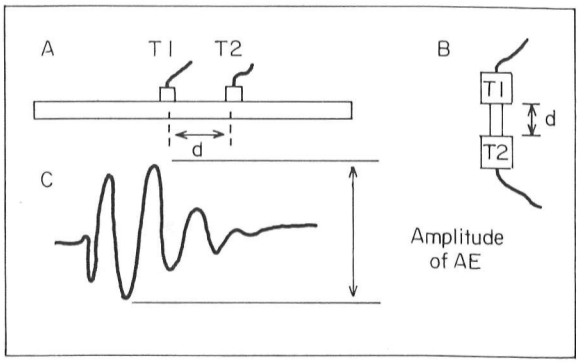

Figure 4. Experimental arrangement for attenuation measurements; 'd' indicates the distance of separation between transducers. (A) Showing placement of two R15 transducers (T1 and T2) on a birch dowel or maple stem. (B) Showing placement of transducers on a pine or *Thuja* block. (C) An AE curve showing the meaning of amplitude.

Relative transducer sensitivity

Signal attenuations were more in pine and *Thuja* than in maple and birch. The effective listening distance for cavitation-induced AEs in pine is of the order of 1 or 2 cm. This fact was used to devise a screening technique to select transducers having the highest signal to noise ratio.

Pine stem segments typically 20 cm long were collected, rehydrated in water and stripped of bark. A reference transducer (PAC model R15) was clamped near the centre of the segment and the comparison transducer was clamped as close to the reference transducer as possible. The gain of the amplifiers attached to each transducer was adjusted until the peak to peak noise was 0.4 V (maximum positive spike 0.2 V); the sample was kept wet so that no cavitation events occurred during the gain adjustment. The pine segment was fully air

dehydrated while counting all AE events having positive going spikes in excess of 0.25 V. The transducer with the largest signal to noise ratio was deemed to be the one recording the largest number of AE events. The relative sensitivity, S_r was computed from the following definition:

$$S_r = \frac{\text{[cumulative AEs of the comparison transducer]}}{\text{[cumulative AEs of the reference transducer]}} \quad (2)$$

The comparison transducers used were: Models N30W, R6, R15 and R80 (all from Physical Acoustics Corp., Princeton, NJ, U.S.A.), model MAC175L (from Acoustic Emission Technology, Sacramento, CA, U.S.A.), model 8312 (from Bruel and Kjaer, Marlborough, MA, U.S.A.), a 'pinducer' (from Valpey-Fisher, Hopkinton, MA, U.S.A.) and the I15I transducer in conjunction with the Drought Stress Monitor built as part of the DOE-SBIR research. All AE events were counted using custom built AE counters of the type described by Tyree & Dixon (1983) and Tyree *et al.* (1984). The pinducer used was one of a lot of 12 and was selected because it had a sensitivity to pencil lead breaks nearest the median of the 12 pinducers.

Results

Velocities

Velocity measurements for AEs travelling axially are shown in Table 1. All velocities range from 2.4 to 6.3 km/s. These figures are all in accord with those reported elsewhere for longitudinal sound propagation in wood (McDonald, 1978; Bucur, 1983).

Frequency composition of AEs

The waveforms of AEs arising from cavitation events tended to have two or three dominant frequency components superimposed. Occasionally, cavitation-induced AEs were predominantly one frequency. The FFT of each AE was computed and the amplitudes of each frequency component of the FFT was normalized to one by dividing each amplitude by the value of the largest. The normalized FFTs of 200 AEs were then averaged and renormalized to one. In Fig. 5 are plots showing the average frequency composition of 200 AEs collected early and late in the dehydration of maple and *Thuja* shoots collected on the Bruel & Kjaer model 8312 transducer. Similar data collected on the Panametrics model V105 are shown in Fig. 6.

Means of 200 AEs were plotted in Figs 5 and 6 to better show long-term trends. Individual AE events tended to be quite variable in frequency composition, i.e. some AEs had predominately low frequencies others predominately high frequencies others were fairly broad-band. There was a tendency for more AEs of high frequency and/or less AEs at low frequency as wood samples dehydrated. During a dehydration experiment, 30–60 sets of 200 AEs were collected and there tended to be a smooth transition from the early to late frequency spectrums as shown in Fig. 6. The trend was less distinct in Fig. 5. The FFTs shown are fully representative of hundreds of data sets. The 95% confidence limits on all means of relative amplitude at any given frequency tended to be ± 0.03 relative units or less. So means that differ by more than about 0.06 relative units are significantly different at better than the 0.99 confidence level.

Comparing Figs 5 and 6 reveals two features: (1) The apparent frequency composition of AE signals obtained by the two transducers differ significantly. (2) Regardless of what transducer is used it appears that the dominant frequency tends to drift a little towards the higher frequencies late in the dehydration period ($> 90\%$ cavitated) than early in the dehydration period ($< 10\%$ cavitated). An increased amplitude of any given frequency between the average FFTs of early and late dehydration periods indicates that there were more AEs having that dominant frequency. Generally, frequencies in the range of 100–300 kHz were dominant or co-dominant in amplitude. The frequency composition measured in *Thuja* was independent of the size of the wood sample dehydrated for samples ranging from 1 cm diameter by 10 cm long to samples 0.05 cm diameter and 0.3 cm long.

Attenuation of AEs

The apparent attenuation of AEs generated by pencil lead breaks was measured on a birch dowel as illustrated in Fig. 7. Transducers T1 and T2 were placed 5 cm to the right and left of the centre of a 90 cm birch dowel 1.33 cm in diameter. Pencil leads were broken at different distances to the right or left or at the centre of the dowel. The attenuation was more for AE sources near the pair of transducers than for sources farther away. The amplitude ratio was one (attenuation = 0 dB), when the AE source was at the midpoint between T1 and T2. The trend indicated by the line in Fig. 7 is approximately symmetrical. Deviations from symmetry were probably because of asymmetrical fibre orientation in

Table 1. Velocity of AE propagation in the longitudinal direction. The source of AEs was a pencil lead break on the cylindrical surface of a dowel (birch) or stem surface (maple and pine)

	Velocity (km/s ± S.E.M.)	
Sample	Stem wet	Stem air dry
Birch	—	6.3 ± 0.1
Maple	4.20 ± 0.02	4.48 ± 0.03
Pine	2.4 ± 0.05	2.78 ± 0.01

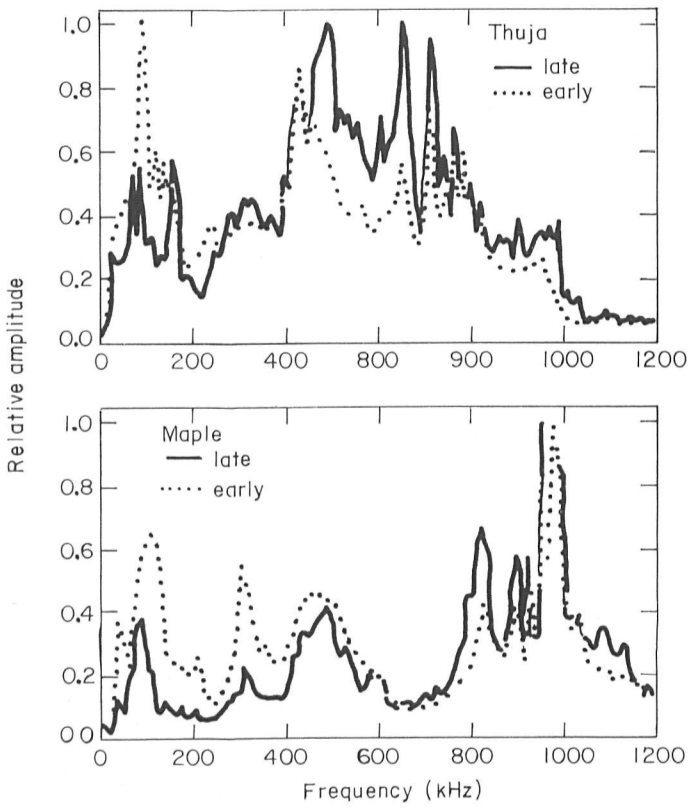

Figure 5. Plots of amplitude versus frequency of cavitation-induced AEs during the dehydration of *Thuja* and maple stems. All plots were derived from a discrete fast Fourier transformation analysis of AEs collected on a Bruel & Kjaer model 8312 transducer. Each plot is the average of 200 AEs. 'Early' and 'late' refer to when during the dehydration the AEs were measured; early means that $< 10\%$ of all AEs had occurred and late means that $> 90\%$ of all AEs had occurred.

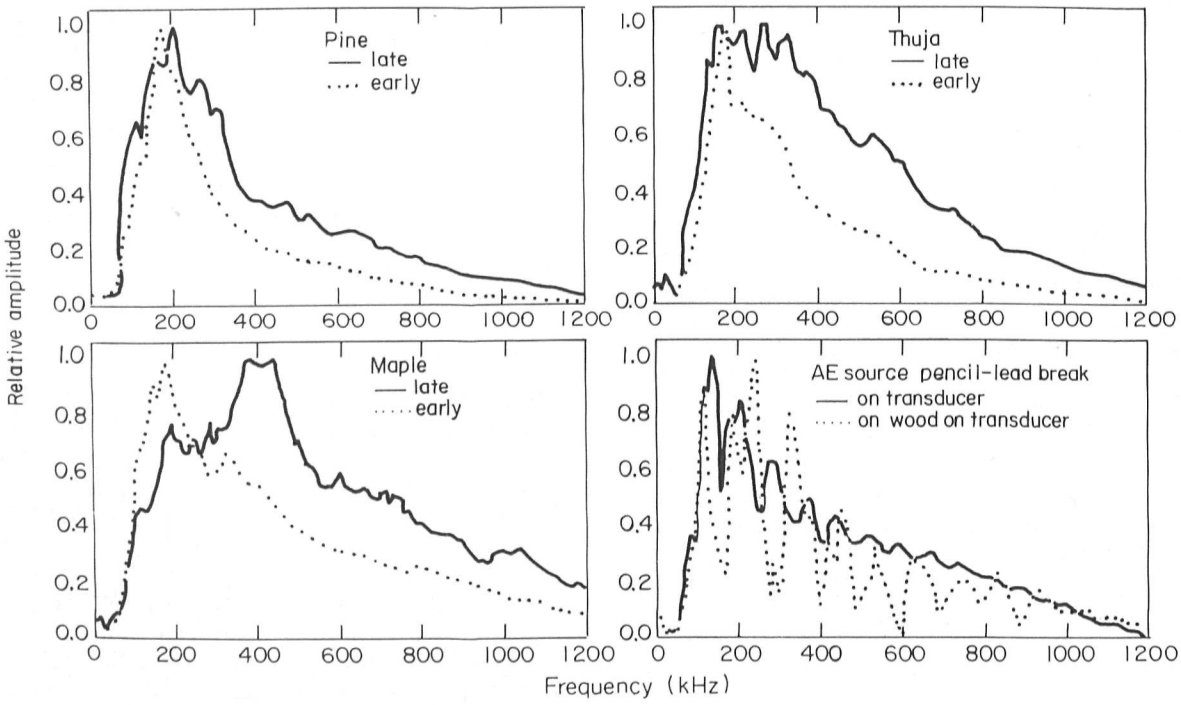

Figure 6. Similar to Fig. 5, but AEs were collected with a Panametrics model V105 transducer. Fourier transformations are also shown for pencil lead breaks directly on the surface of the V105 transducer or on the surface a piece of pine wood mounted on the V105 transducer. The Fourier transformations for pencil lead breaks are for single but representative AE signals.

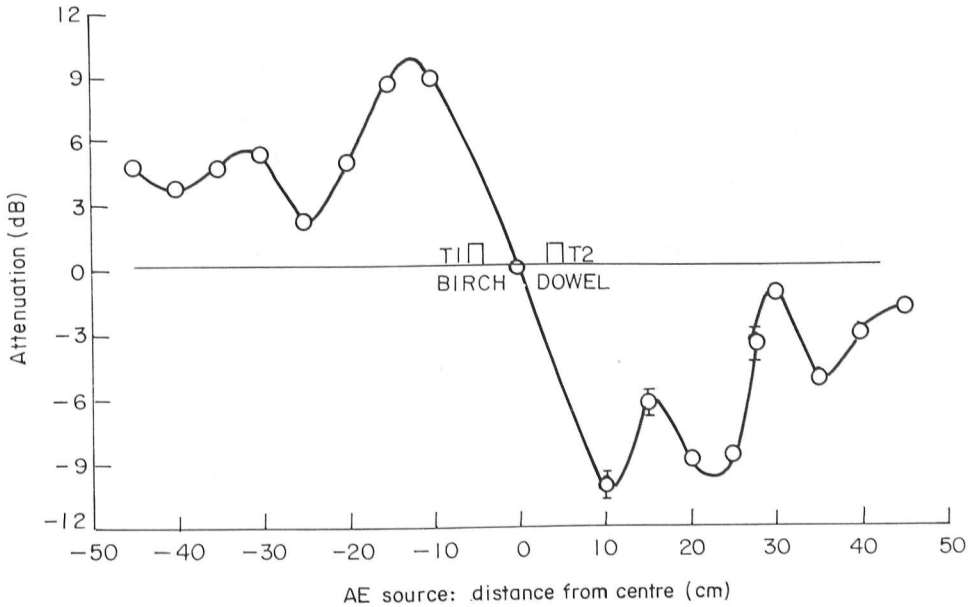

Figure 7. Attenuation measurements in a birch dowel measured for pencil lead breaks at various distances from the centre of the dowel. T1 and T2 show the placement of the two R15 transducers.

the dowel. The velocity of sound differs according to the direction of sound propagation with respect to the fibre orientation, i.e. for longitudinal, radial and tangential directions of propagation in wood samples (McDonald, 1978; Bucur, 1983). The fibre orientation did not follow precisely the long axis of the dowel and the line of cut of the dowel appeared to have been in the vicinity of a side branch (knot). In other experiments, the asymmetrical properties of the dowel were confirmed by placing the transducers farther apart. When the transducers were spaced 50 cm apart (25 cm each side of the midpoint), the amplitude ratio was no longer 1 when the AE source was located at the midpoint between the transducers.

The primary value of this experiment is to illustrate, in the simple geometry of the birch dowel, how AEs tend to bounce off cylindrical surfaces to either reinforce or cancel out to produce different apparent attenuation factors by the time the AEs reach the transducers. If there were only one mode of wave propagation and only one pathway from the source of the AE to the two transducers, then the apparent attenuation would be independent of the distance of the source to the transducers. These results suggest more complex patterns of wave interference. When AEs originate 5 cm from the nearest transducer then the sound wave travelling the shortest route to the transducers tend to cancel out the waves that travel a longer route and reflecting off the opposite surface of the dowel. These effects (as expected) are less significant the further the source of the AE is from the nearest transducer. Qualitatively similar things ought to happen in stems having more complicated geometries.

Attenuation properties ought to be a function of wood hardness and sample geometry. Although maple wood dowels were not available to them for similar experiments, the authors would expect qualitatively similar results for all hardwood samples. Unpublished results on maple stems which tappered in diameter from about 2 to 1 cm diameter over a distance of 1 m confirm this presumption.

Table 2. Specific attenuation values, A_s, measured for AEs from pencil-lead breaks and for AEs from cavitation events. See Appendix 1 for details regarding A_s measured for cavitation events. All measurements apply to the frequency range of 100–300kHz except where indicated. Numbers in brackets give the number of AE sources (pencil-lead break sources) or the number of stem samples dehydrated (cavitation event sources)

	Ranges of A_s dB/cm	
Sample	AE source: pencil break	Cavitation event
Birch	0.2–0.9 (100)	—
Maple	0.3–1.4 (40)	1.1–1.9 (3)
Thuja	5.0–14 (20)	8–12 (3)
Thuja (600–1200 kHz)	—	15–18 (3)
Pine	4–12 (2)	8–20 (3)

A summary of specific attenuations, A_s, appears in Table 2. The range of specific attenuations measured for cavitation-induced AEs tended to be consistently higher than for AEs originating from pencil lead breaks. However, the trends were not strong enough to meet statistical test of significance. Note that in *Thuja* samples the specific attenuation is more for high-frequency AEs than for low-frequency AEs. During the measurement of attenuation for cavitation-induced AEs in pine and *Thuja*, more than 90% of the AEs detected by one transducer were also detected in the other. This suggests that most of the AEs were within listening distance of both transducers. In the maple samples, only about 30% of the AEs detected in one transducer were also detectable in the other. This is about what should have been expected for the experimental configuration (Fig. 4a); most of the stem tissue was beyond the listening distance of both transducers.

Relative sensitivities of transducers

A summary of relative sensitivities of transducers is shown in Table 3. The R15 transducer, used as a reference, was more sensitive than most other transducers. The MAC175L was approximately the same. However, the MAC175L transducers had a potentially serious problem. Spurious AEs could be generated on the AET transducers by gently moving the signal cable. The coupling where the cable entered the body of the transducer appeared to be the source of the problem. The AET transducers were found to be unsuitable for field measurements because wind-induced motion of stems and caused spurious AEs because of the poorly designed cable junction.

The best transducer appeared to be that designed for use on the drought stress monitor (DSM) built as part of the DOE-SBIR project. The I15I transducer as tested with the DSM amplifiers and counting circuit. The authors cannot say at this point if the I15I transducer or the amplifiers (or both) were the source of the superior sensitivity. The previous standard transducer used for cavitation studies was the Bruel & Kjaer model 8312 (Tyree & Dixon, 1983; Sandford & Grace, 1985; Tyree *et al.*, 1986). It can be seen that the new system built by Physical Acoustics is about seven times better in terms of signal to noise ratio.

Discussion

It is difficult to say exactly what the mode of origin and the mode of transmission of the cavitation-induced AEs is in wood samples. From Table 1, it can be seen that the velocity of longitudinal motion of the AEs is about the same in fully hydrated and air-dried wood samples. The velocity of ultrasound in water (1.53 km/s) is much less than that reported in Table 1. The volumetric water content of fully hydrated wood is 0.5–0.8 by volume. So the higher velocities measured strongly suggests that the medium through which the sound propagates is the cellulose material of the cell walls of wood. Thus, the properties of the wood cellulose in combination with the properties of the transducer together determine the frequency composition of the AEs detected.

Ultimately, Table 3 contains the information most pertinent to the selection of transducer types. The other information provides some insight into why the results should be as they are in Table 3.

In all experiments in which S_r was measured, the gains were adjusted until the typical maximum amplitude of the background noise was about 2 dB below the voltage that triggered the detection of an AE event on the event counters. With these settings,

Table 3. Relative sensitivity, S_r, of transducers. The reference transducer in all cases was a model R15. The comparison transducer is listed in the left hand column. A value of S_r more than one indicates that the comparison transducer had a better signal-to-noise ratio for the detection of cavitation events. A ratio less than one indicates that the comparison transducer was inferior. All errors reported are standard errors of the mean. Numbers in brackets are the number of measurements used to compute the means. Band pass filters are indicated by low and high frequency cut off values. High pass filters are indicated as such

Comparison transducer	Filter (kHz)	S_r [Re.: R15 with 100–300 kHz filter]	
R15	100–1200	0.75±0.06 (6)	A,E*
R6	50–200	0.50±0.07 (6)	A,E
MAC175L	125–250	0.91±0.08 (6)	B,E
N30W	200–400	0.48±0.07 (5)	A,E
B&K 8312	100 hi pass	0.185±0.020 (7)	C,E
R80	600–1200	0.09±0.01 (4)	A,E
Pinducer	100 hi pass	0.10±0.02 (4)	A,E
I15I+DSM	100–300	1.37±0.09 (6)	D,F

*Letters refer to amplifier systems used with the transducers. Pre-amplifiers: A=1220A, B= C= B&K 8312 internal, D=I15I internal Post-amplifiers: E=custom built based on LH0032 Op-Amp, F=DSM internal.

the background count rate was in the range of 0.1–0.5 events per minute. The S_r values in Table 3 effectively reflect the frequency dependence of the attenuation properties of the pine samples plus the signal-to-noise ratio of the measuring system, i.e. transducer + filter + preamplifier + post-amplifier. In many cases, the preamplifier and post-amplifiers are the same so that differences reflect the signal to noise ratio of the transducer + filter combinations. It can be seen that the I15I transducer and amplifiers of the drought stress monitor (DSM) developed for the SBIR research contract is superior to all other systems studied. Since the I15I and DSM have unique transducers and amplifiers, it is not possible to say if the improvement lies in the transducer or the amplifier designs.

The R15 with a 100–300 kHz band pass filter is superior to the same transducer with a 100–1200 kHz band pass filter. This is because it was necessary to turn the overall gain down a few dB lower to eliminate the higher frequency noise that the wider band pass filter allowed to pass.

The superior performance of the best three transducers (I15I, R15, and MAC175L) can be attributed to the fact that the typical cavitation-induced AEs have a strong frequency component in the 100–300 kHz range (see Fig. 5). Although frequencies about as strong or stronger sometimes exist in the 400–1200 kHz range, the performance of transducers in the higher frequency bands are inferior for three probable reasons: (1) transducer and/or amplifier noise is worse at the higher frequency ranges, (2) the inherent sensitivity of the transducers is less at the higher frequency ranges, or (3) there is more rapid signal attenuation in wood samples in the higher frequencies (Table 2). The cost of the transducers precluded the possibility of testing a range of transducers of the same model to see if these results are representative of all transducers of the same model. However, all manufacturers have informed us that the transducers supplied were 'representative' of their 'typical' product.

Of considerable significance is the question of whether one can determine the locus of origin of a cavitation-induced AE from the amplitude or frequency composition of the AE signal as received by the transducer. Although some people (Milburn, 1973) have suggested that large xylem conduits store more elastic energy when under sap tension than small conduits, it is clear that amplitude would not be a good indicator of the size of the conduit which is the source of the AE. The AE signals attenuate rapidly (Table 2, Fig. 6) and constructively or destructively interfere as they bounce off surfaces in the stem while travelling *en route* from the source to the transducer.

Others have suggested that large conduits may produce AEs of characteristically longer wavelength than would small conduits, for example, Sanford & Grace (1985). One of the present authors (MTT) must assume responsibility for having either instilled or at least reinforced this idea in the mind of Dr Grace when he worked in MTT's lab in 1983 and viewed some of their early AE signal analyses. The authors no longer subscribe to this dubious hypothesis. They do not know the mode of AE signal propagation in the wood nor the mode of vibrations that conduits might experience. Even if it is assumed that conduit walls might vibrate in and out radially following a cavitation event, the frequency of vibration will depend on all of the following factors: (1) the length between vibrational nodes, (2) the elasticity of the wall, (3) the mass of the wall, (4) the nature of the attachment of the walls to surrounding cells. Two different hypothetical modes of vibration between different fixed nodes are illustrated in Fig. 8. In the first (A), the whole length of the wall of the vessel is shown vibrating in and out. In the second, the nodes of vibration are confined to the location of cross walls of the para-vascular cells (C). In the authors' view, the second mode of vibration (B) is more likely than the first (A) since (A) would require considerable stretching and compression of the cross walls of cells (C).

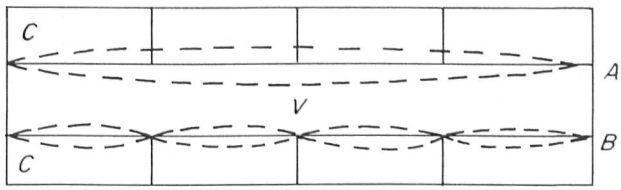

Figure 8. Possible modes of vibration of a vessel (V) wall attached to paratracheal cells (C). The walls are shown in solid line. The dashed line represent possible wall displacements during a mode of vibration. (A) Shows hypothetical vibration along the full length of the vessel requiring distortion of cross walls (bold vertical walls). (B) Shows hypothetical vibration about the nodes formed by cross walls.

There is also positive evidence for the relative importance of wall elasticity and/or mass in determining the characteristic frequency of AEs. In conifers, earlywood tracheids cavitate before latewood tracheids as shown by dye perfusions and other evidence (Tyree *et al.*, 1984; Tyree & Dixon, 1986). This study shows that the AEs have higher frequency components near the end of the dehydration when latewood tracheids cavitate than at the beginning when earlywood tracheids cavitate. But there is no difference in the length of earlywood and latewood tracheids in *Thuja* and pine (unpublished results of tracheid lengths measured on macerated earlywood and latewood tissue).

Finally, there is evidence that the frequency composition of AE signals can be significantly changed when they travel through the wood or through the transducer. A pencil-lead break produces a step-wise decompression of about 0.5 μs duration (Dr Richard Weaver, personal communication). But by the time this short duration AE is received by the transducer, the authors have found it to last 50–

400 μs on the Bruel & Kjaer model 8312 transducer and 10–20 μs on the Panametrics model V105 transducer even when the pencil lead is broken directly on the surface of the transducers (data not shown). This suggests that the frequencies observed are largely the artifact of the transducers themselves. Compare the large difference between the Fourier transformations of AEs from *Thuja* and maple collected on the Bruel & Kjaer transducer (Fig. 5) and the Panametrics transducer (Fig. 6). By comparing the Fourier transformations resulting from a pencil-lead break directly on the V105 transducer to the Fourier transformation for a pencil-lead break on a pine wood sample resting on the V105 transducer, it can also be seen that the wood also alters frequencies received. Certain frequencies are selectively removed and others appear to be enhanced. The possibility that earlywood tissues remove more lower frequency signals when air filled late in the dehydration than when water filled early in the dehydration cannot be discounted. The authors feel it is premature to conclude anything about the locus of origin of AEs based solely on frequency compositions of raw Fourier transformations.

As a consequence of this work and of the collaborative efforts of Physical Acoustics Corp., an AE counter has been designed for commercial distribution, the model 4615 Drought Stress Monitor (DSM). Some useful features of the device are: (1) it is small, light weight and battery powered, (2) it has a seven times better signal-to-noise ratio than systems previously used in the authors' laboratory, (3) it is microprocessor controlled and programmable, (4) it will log AE data in memory and dump it to a host computer for further analysis. One of the authors (MTT) has written software to allow an IBM-PC or clone to communicate with, program, dump and plot data from the 4615 DSM and is available at no cost.

Acknowledgments

This work was made possible by a subcontract from Physical Acoustics Corp. who also provided the loan of some equipment used and provided much useful advice. Some transducers, the waveform digitizer and the computer used in this study were purchased with an equipment grant from the Natural Sciences and Engineering Research Council of Canada (NSERC). Some of the Fourier transformations reproduced here were obtained in 1985 while MTT was at the University of Toronto and funded by NSERC grant number A6919. We also thank Dr Richard Weaver, University of Illinois, who is a noted expert on the theory of ultrasound propagation in metals, for many long and valuable discussions. Dr Weaver summarized for us many significant concepts derived from diverse papers too technical and mathematical for us to understand. Mel Tyree must assume full responsibility for any distortions of theory or fact that may result from our simplified discussion of the concepts explained to us by Dr Weaver.

References

Bucur, V. (1983) An ultrasonic method for measuring the elastic constants of wood increment cores bored from living trees. *Ultrasonics*, **21**, 116–126.

McDonald, K.A. (1978) Lumber defect detection by ultrasonics. Research Paper FPL 311. Forest Products Laboratory, Forest Service, USDA, Madison, Wis.

Milburn, J.A. (1973) Cavitation in *Ricinus* by acoustic detection: Induction in excised leaves by various factors. *Planta*, **110**, 253–265.

Pena, J. & Grace, J. (1986) Water relations and ultrasound emissions of *Pinus sylvestris* L. before, during and after a period of water stress. *New Phytologist*, **103**, 515–524.

Sandford, A.P. & Grace, J. (1985) The measurement and interpretation of ultrasound from woody stems. *Journal of Experimental Botany*, **36**, 298–311.

Salleo, S. & LoGullo, M.A. (1986) Xylem cavitation in nodes and internodes of whole *Chorisia insignis* H.B. et K. plants subjected to water stress: relations between conduit size and cavitation. *Annals of Botany*, **58**, 431–441.

Tyree, M.T. & Dixon, M.A. (1983) Cavitation events in *Thuja occidentalis* L.? Ultrasonic acoustic emissions from the sapwood can be measured. *Plant Physiology*, **72**, 1094–1099.

Tyree, M.T. & Dixon, M.A. (1986) Water stress induced cavitation and embolism in some woody plants. *Physiologia Plantarum*, **66**, 397–405.

Tyree, M.T., Dixon, M.A. & Thompson, R.G. (1984) Ultrasonic acoustic emissions from the sapwood of *Thuja occidentalis* measured inside a pressure bomb. *Plant Physiology*, **74**, 1046–1049.

Tyree, M.T., Fiscus, E.L., Wullschleger, S.D. & Dixon, M.A. (1986) Detection of xylem cavitation in corn under field conditions. *Plant Physiology*, **82**, 597–599.

Appendix

Attenuation of ultrasonic acoustic emissions in wood

In this analysis, the authors start out with several simplifying assumptions that are needed to arrive at a way of calculating a specific attenuation factor, A_s. These assumptions serve to produce a relatively simple set of equations. Later, they will discuss how the real situation will modify the expected theoretical behaviour. The simplifying assumptions are:

(1) The AE amplitude attenuates exponentially with distance travelled down the stem. (This assumption is correct for plane waves moving through an infinite medium; waves attenuate because of visco-elastic energy loss.)
(2) Attenuation is approximately independent of the range of frequencies contained in AE waves.
(3) The distance the AE waves travel is much longer than the diameter or thickness of the wood sample.
(4) The AE transducers makes a point contact with the wood sample, i.e. the size of the transducer is small compared to the separation between the two transducers.

Pencil-lead break as a source of known locus (Fig. 9a)

Consider transducers T1 and T2 separated by a distance d and AE signal sources at B1 or B2 at any distance beyond but not between the transducers. If the AE signal level at the source is L_o, it will decline, by assumption, exponentially with distance away from the source:

$$L = L_o\, 10^{-Kx} \qquad \text{(A1)}$$

where L is the signal level at distance x, cm, from the source and K is the an attenuation constant. For a source at B1 the signal level at TR1 and TR2 are:

$$TR1 = L_o\, 10^{-KD} \qquad \text{(A2a)}$$

and

$$TR2 = L_o\, 10^{-K(D+d)}, \qquad \text{(A2b)}$$

where D is the distance from B1 to T1, d is the distance between T1 and T2, and TR1 and TR2 are the AE amplitudes at T1 and T2, respectively, as in Eqn (1). Dividing Eqn (A2a) by Eqn (A2b), taking the log of both sides of the result, and multiplying the result by 20 (to get dB units) yields the attenuation factor A in Eqn (1):

$$A = 20 \log[TR1/TR2] = 20Kd. \qquad \text{(A3)}$$

From this, it is clear that A is related to the product of K and d and it also follows that the specific attenuation defined in the 'Materials and methods' section is given by

$$A_s = A/d = 20K. \qquad \text{(A4)}$$

From Eqns (A3) and (A4) it can be seen that the distance of the source of the AE from the transducer pair is unimportant in the calculation of A and A_s. For a source located at B2, the sign but not the magnitude of A and A_s will change.

The relationships developed here are only crude approximations of the real physical situation in which attenuation factors are measured. The use of an 8-bit waveform digitizer poses serious limitations because of its narrow dynamic range (48 dB). To assure an accurate value of TR1/TR2 it is necessary to keep the ratio in the range of 20 dB and the minimum amplitude over 20–30 dB so that the maximum amplitude is also within range of the digitizer. For the maple and birch samples this meant that T1 and T2 could be separated by only about 5–10 cm which is not much more than the diameter of the R15 transducers (1.8 cm). Since there is some uncertainty regarding where along the transducer the AE enters the transducer the evaluation of d is uncertain. There are a number of other confounding factors including: (1) The AEs are not all of the same frequency and frequently have several frequency components. Since visco-elastic attenuation is a function of frequency the waveform and amplitude is distorted as the wave travels (in water the attenuation constant, K, is inversely proportional to the square root of the frequency). (2) There are two modes of wave propagation in solids: one is a compression wave and the other is a surface wave. These waves travel at different velocities, the surface wave being about twice the velocity of the compression wave. These waves travelling at different velocities will interfere with each other sometimes nullifying each other and sometimes reinforcing each other. (3) As the waves propagate through the medium, some components of the waves will reflect off the surfaces of the wood and internally where large density changes are encountered. The reflected waves, having travelled a longer distance will also interfere with the waves that have followed the most direct path from the source to the transducers. The ultimate result of all wave interference is that the waves will not decline exponentially with distance. At some locations, the wave amplitude will be much larger than expected and at other points will be much smaller in amplitude than predicted by the simple theory above. (4) The transducers themselves will modify the waveforms as the waves bounce around inside the body of the transducer and because harmonic frequencies characteristic of the transducers will make some transducers ring on long after the AE has ceased in the wood sample.

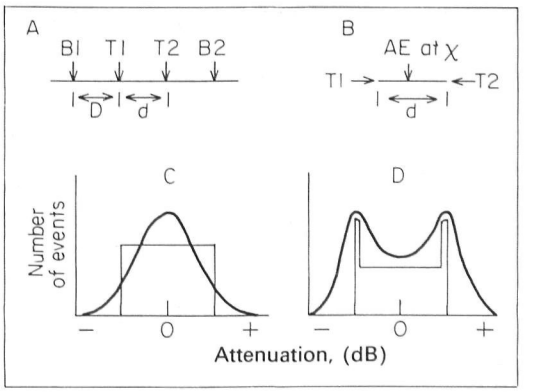

Figure 9. Theory of attenuation measurements. (A) experimental set up where transducers T1 and T2 are separated a distance, d cm, apart near the centre of a stem segment. B1 and B2 show places where leads might be broken. (B) experimental set up where transducers T1 and T2 are at the ends of a stem segment d cm long. (C) Theoretical curves of number of AEs versus attenuation for case B. (D) Theoretical curves of number of AEs versus attenuation for case A. See Appendix 1 for details.

Attenuation of AEs from an unknown locus

Pine and *Thuja* samples had a large specific attenuation. In order to measure attenuation of AEs from cavitation events, small blocks of length, d, were clamped between two matched transducers. This situation in illustrated in Fig. 9b. Consider an AE at some arbitrary distance x from T1. Using an argument similar to that above it can be shown that the measured attenuation will be given by

$$A = 20 \log[TR1/TR2] = -K(2x - d). \qquad \text{(A5)}$$

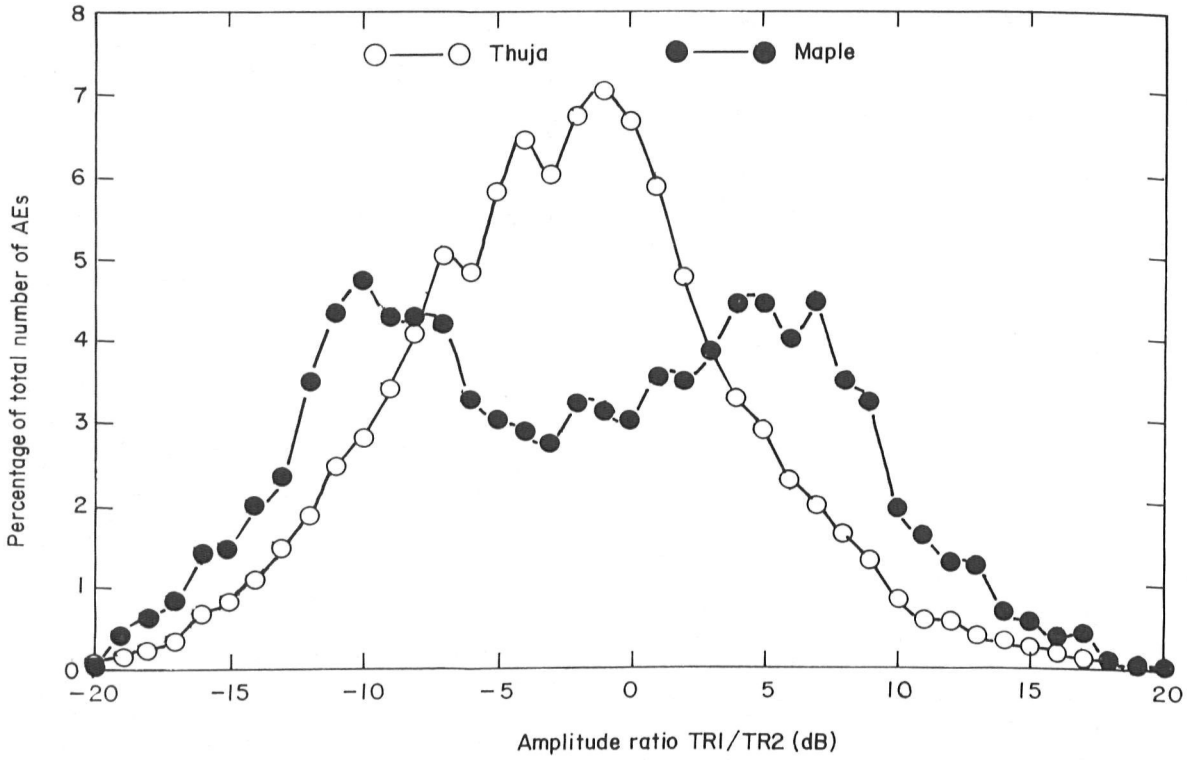

Figure 10. Actual attenuation curves for AEs from cavitation events in maple and *Thuja* stems. The *Thuja* curve is for the experimental set up in Fig. 7B using R80 transducers (600–1200 kHz filter). The maple curve is for the experimental set up in Fig. 7A using R15 transducers (100–300 kHz filter). In the maple experiment, the transducers were separated by 4 cm. In the *Thuja* experiment, the transducers were separated by 0.4 cm.

Note that when the AE originates in the centre ($x = d/2$) that $A = 0$ dB. Also the maximum and minimum values of A occur when $x = 0$ and $x = d$, respectively. Although the authors do not know where any one AE occurs, it is very likely that the occurrence of AEs will be more or less evenly distributed overall possible x values during the course of a dehydration. The maximum and minimum values of A can be determined from a frequency histogram of the number AEs versus the attenuation value from which values of K and A_s can be evaluated. The expected histogram is illustrated in Fig. 9c, thin solid line.

On maple samples the transducer could be spaced 5–10 cm apart in the middle of stem segments 50 cm long. This case is illustrated in Fig. 9a. The only difference here is that AE outside of the space between the two transducers will yield the maximum or minimum values of A. The expected frequency histograms are given in Fig. 9d, thin solid line.

When account is taken of the reality of the situation (large transducers, internal reflection of AEs, interference and the frequency dependence of K) then the expected histograms would probably look like the thick lines in Fig. 9c and d. Two examples of actual experimental data are shown in Fig. 10.